공학석사 학위논문

히알루론산- 인산칼슘 나노 복합체 하이드로겔의 제조 및 평가

Hyaluronic acid – calcium phosphate nanocomposite hydrogel via *in-situ* precipitation process

2014년 2월

서울대학교 대학원

재료공학부

정설하

Abstract

Hyaluronic acid – calcium phosphate nano composite hydrogel via *in-situ* precipitation process

Seol-Ha Jeong
Department of Materials Science and Engineering
Seoul National University

Hyaluronic acid (HAc) exhibits excellent biocompatibility and hydrophilicity, whereas it has limitations on biomedical applications due to poor biomechanical properties as well as fast in vivo degradation through enzymatic degradation. In this study, we have introduced in-situ precipitation method for fabrication of HAc-calcium phosphate (CaP) nanocomposite hydrogel in order to improve mechanical and biological behaviors of HAc under physiological conditions precipitating calcium phosphate nanoparticles. In particular, in-situ precipitation facilitates homogeneous and

fast incorporation of nanoparticles into a polymer matrix. The nanocomposite hydrogels with various CaP content were fabricated and then evaluated to find optimal conditions of the hydrogels. The CaP nanoparticles were distributed homogeneously within HAc matrix, increasing surface roughness of the hydrogels, and appeared uniform with the size of ~200 nm. The degradation of the composite hydrogels was significantly retarded as compared to that of pure HAc hydrogels in hyaluronidase solution, showing improved chemical stability of the composite. Moreover, composite hydrogels exhibit improvement on rheological behaviors, indicating the shear moduli of composite hydrogels are 2.5-4 times as great as pure HAc hydrogel depending on the CaP content. Furthermore, fibroblast cells on the nanocomposite hydrogels showed more advanced progress of cell adhesion as compared to HAc hydrogel. The level of cell proliferation behaviors on nanocomposite hydrogels after 5 d was around 8 times higher than that on HAc hydrogel, implying the enhanced biocompatibility of composite

hydrogels. By controlling the CaP amounts, mechanical and biological behaviors of the nanocomposite hydrogel can be optimized, exhibiting great potential for various biomedical applications.

Keywords: Hyaluronic acid (HAc), Precipitation, Calcium Phosphate, Nanoparticles, Biocompatibility

Student Number: 2012-20632

Content

List of Tables

List of Figures

Chapter 1. Introduction

1.1. Hydrogels as tissue engineering materials

Polymer scaffolds serve a significant role in the tissue engineering applications based on their structural and biochemical properties. The materials for the biomaterial scaffolds require certain properties such as biocompatibility, biodegradability, and biomechanical stability. In other words, the scaffold must be designed to promote cell proliferation and differentiation that lead to tissue formation and to be biodegradable which approximates the rate of tissue generation [2, 3].Therefore, many studies on the surface of the scaffolds have been carried out to have certain topographical patterns which can induce cell growth or to be functionalized with growth factors, proteins and DNA [4].

For the tissue engineering scaffolds, hydrogels are the most attractive scaffolds due to their structural and functional similarities to the natural extracellular matrices (ECM). Hydrogels are defined as interconnected networks of macroscopic dimensions, consisting of hydrophilic blocks that

are rendered insoluble due to the presence of crosslinks [1].

1.2. Hyaluronic acid

Hyaluronic acid(HAc) is a biodegradable, biocompatible, and natural linear polysaccharide with various range of molecular weight from 1000 to 10,000,000 Da. HAc is composed of alternating disaccharide units of D-glucuronic acid and N-acetyl-D-glucosamine with β interglycosidic linkage (Fig. 1)[5]. It is naturally derived, enzymatically degradable and non-immunogenic [6]. It is abundant in synovial fluid and ECM and acts not only to control tissue hydration but also to lubricating of synovial joint fluid and vitreous humor in the eye. It plays major roles in wound healing, and in promoting cell motility and differentiation during development [7].The largest amount of HAc resides in skin tissue [8]. HAc is a polyanionic polymer at physiologic pH and is therefore highly charged. The highly charged nature renders it soluble and allows it to bind water extensively [9]. Due to its various functions and physiochemical properties, HAc and

modified HAc have been extensively investigated and used for the treatment of arthritis, ophthalmic surgery, drug delivery, and tissue engineering [5].

However, in its natural state, HAc has poor biomechanical properties as well as fast *in vivo* degradation through enzymatic reactions. Thus, chemical modification or cross-linking to form HAc hydrogel material is required to improve its mechanical properties.

For fabricating the hydrogel, the chemical modification of HAc typically involves the carboxylic groups and/or the alcohol groups of its backbone. The carboxylic acid groups have been modified by esterification and cross-linked via dihydrazide, dialdehyde, or disulfide crosslinkers. Moreover, HAc has been photo-cross-linked by modifying the carboxylic acid groups with methacrylamide [4]. A various crosslinking methods are introduced to synthesis HAc hydrogels using distinct functional groups on HAc as the reactive sites as shown in Fig. 2 and table 1.

1.3. Composite hydrogels

There have been many attempts to improve the mechanical properties of polymeric materials by incorporating inorganic particles which can act as multifunctional cross-linkers [10]. It was demonstrated that nanocomposite hydrogels enhanced the mechanical properties as well as cell growth on materials made of poly (N-isopropylacrylamide) and synthetic silicate nanoparticles [11]. The silicate nanoparticles serve a role as a cross-linker which leads to physical toughness. Gaharwar et al. also developed a silicate cross-linked poly (ethylene oxide) (PEO) nanocomposites with enhanced bioactivity and in vitro cell adhesion properties [12-15].

Among those approaches to fabricate hydrogel networks with excellent mechanical properties using nanoparticles for reinforcement, incorporating hydroxyapatite nanoparticles are one of the excellent candidates for the biomedical application. Since hydroxyapatite is a biocompatible, bioactive and non-immunogenic material, it has been widely

used in the fabrication of polymer composites. However, conventional composite hydrogels with hydroxyapatite are usually formed through simple physical mixing and biomimetic methods [16]. These approaches suffer from low efficiency of mineralization and mechanical improvements [17].

1.4. The aim of this study

In this study, we have introduced in-situ precipitation method for fabrication of HAc-calcium phosphate (CaP) nanocomposite hydrogel in order to improve mechanical and biological behaviors of HAc under physiological conditions by adding calcium phosphate nanoparticles. We evaluate the effect of nano CaP on the structure and mechanical properties of the HAc hydrogels. The scheme of the aim of this study is depicted in Fig. 3.

Table 1. The main strategies for HAc crosslinking presented to date in patent reports and scientific literature (Biotechnological production and application of hyaluronan)

HA group involved	Crosslinking agent	Product	Reference
Carboxyl	Bis-carbodiimide	HA crosslinked via N-glucuronil urea or O-glucuronil iourea groups	Sadozai et al., 2005
	Polyvalent hydrazide coupled with carbodiimide and co-activator	HA crosslinked via hydrazide bonds	Bulpitt et al., 1999; Prestwich et al., 1998
	Carboiimide _ coactivators(sulfo	HA auto-crosslinked via	Radice et al., 2002; Young et al., 2004

	NHS/HOBt) or CMPI	ester bonds	
	Ditiobishydrazide coupled with carbodiimide	HA disulfide-crosslinked via air oxidation	Shu et al., 2003
	Metacrylating agent coupled with carbodiimide	HA photocrosslinked after exposition to light	Leach et al., 2003; Park et al., 2003
Hydroxyl	di-epoxide	HA crosslinked via ether bonds	Balazs et al., 1986 Larsen et al., 1993, Ibrahim et al., 2010
	Divinyl sulfone	HA crosslinked via ether bonds	Balaz et al., 1986, Larsen et al., 1993, Ibrahim et al., 2010

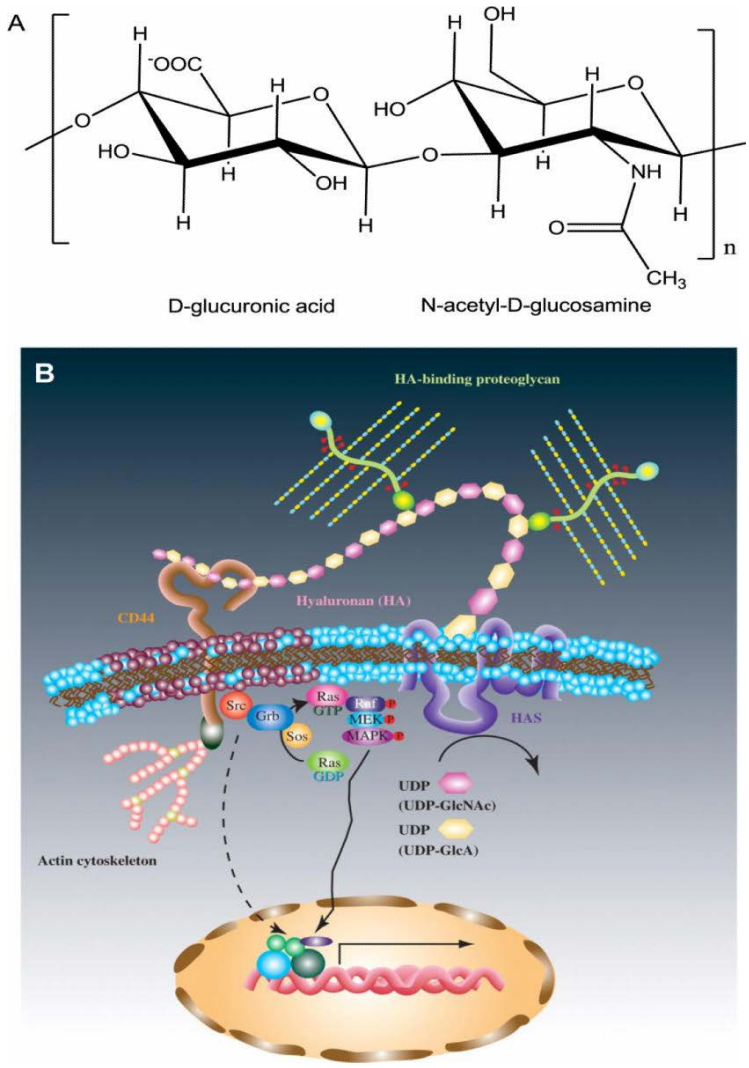

Figure 1. (A) The chemical structure of Hyaluronic acid (Glucuronic acid and N-acetyl-glucosamine) and (B) The function of HA in cellular response.

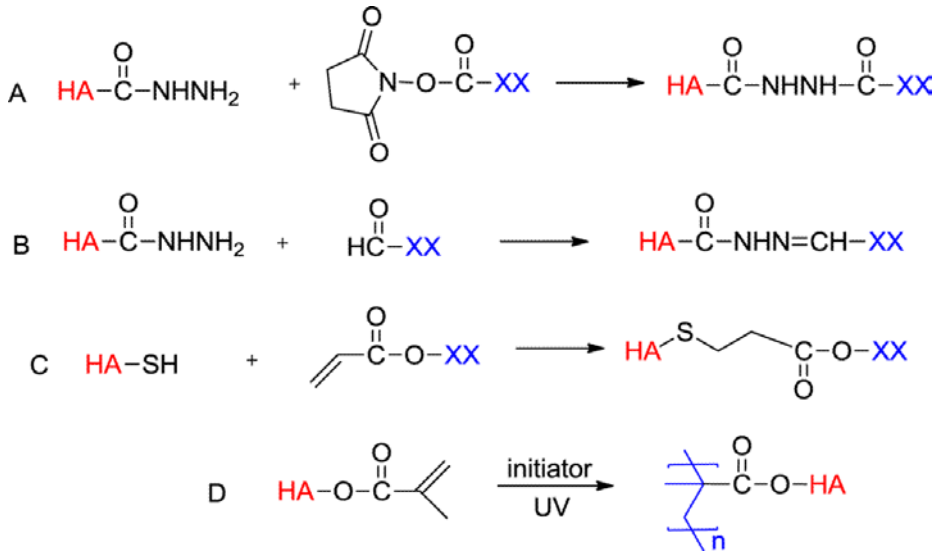

Figure 2. Crosslinking schemes for the synthesis of HAc hydrogels.[1]

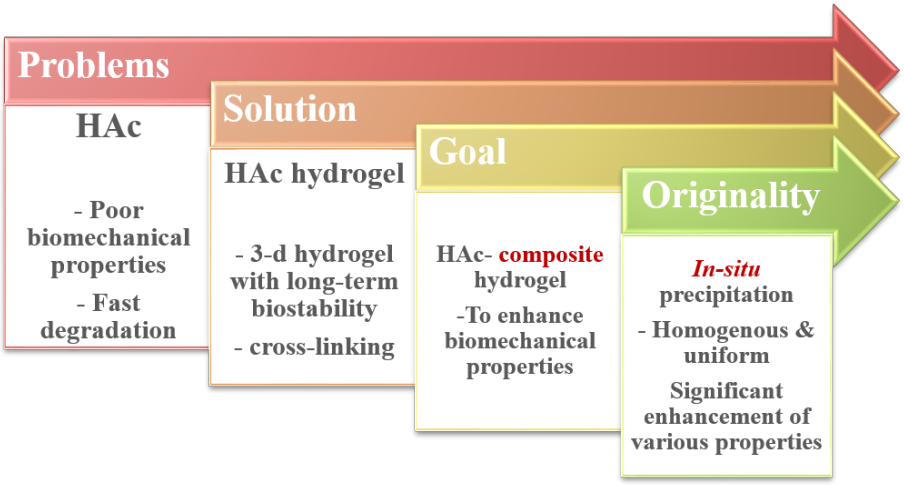

Figure 3. Scheme of the aim of this study.

Chapter 2. Fabrication and evalution of HAc-Cap nano composite hydrogel via *in-situ* precipitation process

2.1. Experimental procedure

2.1.1. Sample preparation

Hyaluronic acid with a molecular weight (MW) of 3000kDa was supplied from Genoss Co. (Suwon, Korea) which was fermented by Streptococcus zooepidemicus.

Cross-linked hydrogels based on photocrosslinking were synthesized according to a protocol modified from Leach et al. creating bonds between glycidyl methacrylate-hyaluronic acid (GMHA) conjugates and N-vinyl-pyrrolidinone.

1 g of HAc was dissolved in 100ml phosphate-buffered saline (PBS) to get a solution of 1 wt % of HAc. Then, 2.2 ml triethylamine, 2.2 ml glycidyl methacrylate, and 2.2 g tetrabutylammonium bromide were added by stages while stirring. After stirred overnight at room temperature, it was precipiatated in acetone. The GMHA conjugates obtained were dissolved again in 100 ml distilled water. To synthesize UV photocrosslinking HAc hydrogels, 5 ml N-

vinyl-pyrrolidionone and 0.1 g of a photoinitiator were gradually added to the GMHA solution. Then, 400 ul of the solution was transferred to the plastic mold with 14 mm diameter and exposed to UV light for 15 minutes. (Wavelength 365nm)The hydrogels were dialyzed in PBS for 48 h to remove remnants of the cross-linkers [18].

2.1.2. Fabrication of Calcium Phosphate-HAc nanocomposite hydrogel

The fabricated HAc hydrogels were immersed in the mixed solution with calcium chloride and phosphoric acid with the ratio of 1.67 for 1 d. Then they were dipped in 15% ammonium hydroxide solution for 3 h to precipitate calcium phosphate within the hydrogels. The hydrogels were dialyzed in PBS for 48h to remove remnants of ammonium hydroxide solution. The nanocomposite hydrogels with various CaP content from 10 wt % to 40 wt % were fabricated.

2.1.3. Characterization

Scanning electron microscopy analysis

Morphology of the composite hydrogels was observed using field-emission scanning electron microscopy (FE-SEM, SUPRA 55VP, Carl Zeiss Co., Germany). In brief, the samples were frozen at -80℃ and then freeze-dried to maintain the samples' structure itself.

Chemical composition analysis

The chemical composition of calcium phosphate was analyzed using an X-ray diffractometer (XRD, D8-Advance, Bruker Co., Germany). The XRD data were obtained from 20 ° to 60 ° (2θ) using CuK_{α} radiation with a scan rate of 1°/min. The samples with three different conditions were prepared for XRD. The original HAc hydrogel, the composite hydrogel, and the composite hydrogel with heat treatment at 1100 ℃ for 5minutes were prepared. The heat treatment was required to remove HAc polymer and to verify that the precipitated particles were calcium phosphate.

The size analysis

The size analysis of nanoparticles in the hydrogels was evaluated by Transmission electron microscopy (TEM, Tecnai F20, FEI Co., USA).

TGA analysis

The CaP content were calculated experimentally using thermal gravity analysis (TGA, Simultaneous DTA/TGA analyzer, TA instruments Co., USA). The original hydrogel and the composite hydrogels with various CaP content were completely dried at air and analyzed by TGA under the condition up to 1100 ℃ and 10 ℃/min. The relative amounts of the remnants were calculated.

Equilibrium swelling ratio

The swelling behaviors of the hydrogels were evaluated at 37 ℃, in PBS. First, HAc hydrogels and the composite hydrogels were dried in a vacuum oven and weighed. Then they were immersed in PBS for 1 day, and then re-

weighed. The water content of the hydrogels was calculated according to

$$\text{water absorbance} = \frac{W_f - W_i}{W_i} \times 100\ (\%) \quad (1)$$

Where W_f represents the weight of the hydrated hydrogel and W_i that of the initial dried hydrogel. Three samples were tested for each CaP content, and the average value was used.

In vitro enzymatic degradation

In vitro degradation tests of the hydrogels were performed in PBS at 37 ℃ with hyaluronidase(HAase) (Type I-S, lyophilized powder, 400-1000 units/mg solid). The HAase was purchased commercially from Sigma Co., Korea. It was dissolved in PBS. Each dried sample was weighed initially and then placed in a 0.05 wt % solution of HAase, and incubated at 37 ℃ for 4 h. The remained samples were extracted and re-weighed after completely dried at air. The percent degraded weight was calculated according to

$$\frac{W_i - Wf}{W_i} \times 100\ (\%) \quad (2)$$

Three samples were tested for each CaP content, and the average value was used.

Rheological behavior tests

Mechanical behavior of hydrogels was assessed using a controlled strain rheometer(ARES, Rheometric Scientific, USA). The hydrogels with the size of 25ϕ, 2 mm thickness were prepared. Those samples were placed on a bottom plate and an were fixed by an upper plate with the normal force 10 N. Frequency sweeps were carried out using parallel plates geometry with 25 mm diameter plates and 2 mm gap to measure the storage modulus, G'. The range of angular frequency was from 0.1 to 100 rad/s at a strain in the linear region. And the temperature of the both plates were set at 37 ℃ while the test. The schematic diagram of the strain rheometer is shown in Fig. 4. Three samples of the pure hydrogel and those of the composite hydrogels were tested for each CaP content, and the average value was used. After measuring,

all the samples were immersed in PBS at 37 ℃ for 24 h to make them fully swollen. The mechanical test was carried out again with the swollen samples following the previous method.

***In vitro* cell tests**

A fibroblast cell line, L929 (derivative of strain L, Mus musculus, mouse), was used to assess the cellular responses on the hydrogels. Prior to the cell seeding, the samples were washed with 70 % ethanol and PBS and sterilized on a clean bench under UV irradiation. The pre-incubated cells were seeded on the hydrogels at densities of 5×10^4 cells/mL (for the cell attachment), 2×10^4 cells/mL (for the cell proliferation), and 1×10^4 cells/mL (for the cell penetration). The cells were cultured in a medium, with an alpha-minimum essential medium (α-MEM, Welgene Co., Ltd., Korea) that was supplemented with 10 % fetal bovine serum (FBS) and 1 % penicillin-streptomycin in a humidified incubator with 5 % CO_2 at 37 °C.

The attached cells were observed using confocal laser scanning microscopy (CLSM, FluoView FV1000, Olympus, Japan) after culturing for 3d. After 3 d, the cultured cells on the samples were fixed in 4 % paraformaldehyde in PBS for 10minutes, washed 3 times in PBS, permeabilized with 0.1 % Trion X-100 and 1 % BSA in PBS for 5min, for 30min, respectively. Then, they were stained by fluorescent phalloidin for 20min. The stained samples were placed on a cover slide with DAPI staining immediately and the cell morphology was observed.

The level of cell proliferation was measured after culturing 3, 5 d using an MTS assay (CellTiter 96 Aqueous One Solution, Promega, USA).

The cell penetration was observed by confocal laser scanning microscopy (CLSM). After culturing for 10d with density of 1×10^4 cells/mL, the hydrogels were immediately frozen by N_2 gas and cut by the blade. The cross sectional plane of the hydrogels were observed for the cell penetration depth. I*n vitro* cell tests were performed three times, and the experimental results were

expressed as the mean ± standard deviation (SD). The difference between the two groups was determined using a one-way analysis of variance (ANOVA), and a $p < 0.05$ was considered statistically significant.

***In vivo* animal tests (preliminary)**

The *in vivo* animal tests were conducted using female rats (12 weeks old, average weight 500 g). The original HAc hydrogel and the 30wt % of composite hydrogel were used in this study. The animals were given a general anesthetic using a combination of 0.07 cc of 2 % Xylazine HCl (Rompun, Bayer Korea, and Korea) and 0.14 cc of Tiletamine HCl (Zoletil, Virbac lab, France) and Lidocaine (Yuhan Corporation, Korea). Additionally, 1:100,000 epinephrine was injected as the local anesthesia. The hydrogels were implanted under the pockets on the dermis of the rats that were cut by blade. The samples before and after implantation were shown in Fig. 5. After the surgery, the wounds were sutured with Surgisorb (Samyang Ltd, Korea), and

then cephradine (Bayer Korea, Korea), an antibiotic, was injected into the rats for 1 d.

The rats were sacrificed 2 weeks and 4 weeks after surgery. The extracted samples with skin tissue were fixed in a neutral 10 % formaldehyde solution, and the tissue blocks were formed using paraffin. The blocks were cut into sections around. The microscopic images of the trichrome and haematoxylin–eosin stained sections were obtained using Axioskop microscopy (Olympus BX51, Olympus Corporation, Tokyo, Japan) at a 100x magnification.

2.2. Results

2.2.1. Fabrication and characterizations of the nanocomposite hydrogels

It was noticed that the composite hydrogels became opaque, indicating the precipitation of calcium phosphate within the hydrogels as shown in Fig. 6. The transparent nature of the HAc hydrogel enabled to monitor the progress

of the precipitation. In Fig. 7, SEM images of the pure HAc hydrogel and the nanocomposite hydrogels revealed differences in their microstructures. In Fig. 7(a) and (b), the pure HAc hydrogel showed smooth and porous structures with pore sizes of around 100 μm. In contrast, the nanocomposite hydrogel showed rough networks with smaller pores according to Fig. 7(c). In the higher magnitude (Fig. 7 d), it was observed that CaP nanoparticles were homogeneously distributed within HAc matrix, and appeared uniform with the size of ~200 nm. In Fig. 8 (left), the cross sectional image of the simply mixed composite hydrogels revealed that the CaP particles were agglomerated during gelation via UV irradiation. The particles were inhomogeneously distributed on the polymer matrix with low dispersity. In Fig. 8 (right), the nano composite hydrogels by precipitation process showed uniformly entangled particles on all area of the polymer matrix. Precipitated nano particles came to the surface of the polymer matrix in comparison to the simply mixed one.

The chemical composition of the nanocomposite hydrogels was confirmed using the XRD in Fig. 9. In the XRD pattern, no characteristic peaks of the original HAc hydrogel were found. The composite hydrogel showed broad peak between 32 ° and 35 °, indicating that precipitated products with the low crystallinity were formed in the composite hydrogel. Strong peaks of the composite hydrogel after heat treatment were observed. Two different calcium phosphate products were identified, beta $Ca_2(PO_2)_7$) and beta- $Ca_3(PO_4)_2$. Both calcium phosphates had around 1.5 Ca/P ratios.

In Fig. 10, the size and chemical composition of the precipitated calcium phosphate particles were analyzed by TEM and EDS respectively. Two distinguishable particles were shown in Fig. 10. Beside the dark round shapes of the particles with 200 nm size, much smaller particles were aligned directionally. 200 nm particles were analyzed with EDS to confirm that it composed of Ca, O and P.

The amount of CaP was calculated experimentally by TGA analysis.

Various concentrations of calcium chloride and phosphoric acid solution were prepared and calculated the relative amount of the remnants after TGA. In Fig. 11, the pure hydrogel showed two curvatures indicating that certain chemical bonding was broken at high temperature.

2.2.2. Equilibrium swelling ratio

The swelling behaviors of the pure HAc hydrogel and the nanocomposite hydrogels were illustrated in Fig. 12. The swelling ratio of the pure HAc hydrogel was 7000 % in average and the hydrogels without undergoing the ion permeation process showed significant high equilibrium swelling ratio, 22200 %. The percent water content in the nanocomposite hydrogels decreased from 11000 % to 2400 % as the CaP amount increased from 10 wt % to 40 wt %, due to the interruption of CaP particles. It is concluded that the swelling degree of the nanocomposite samples are strongly dependent on the CaP concentration. This is attributed to the decrease in the binding sites for water molecules due to the existence of CaP particles

entangled on the HAc matrix.

2.2.3. *In vitro* enzymatic degradation

The overall remained weight after the degradation of the samples in PBS containing 0.05 wt % hyaluronidase is shown in Fig. 13. The enzymatic degradation of HAc results in the cleavage of internal beta-N-acetyl-D-glucosaminidic linkages [19]. In general, the swollen networks of the hydrogels decrease in size when they are exposed to the hyaluronidase throughout the degradation. The degradation of the composite hydrogels was significantly retarded as compared to that of pure HAc hydrogels in hyaluronidase solution, proving the improved chemical stability of the composite. Only 60 % of the pure HAc hydrogels remained whereas 80 % of nanocomposite hydrogels containing 30 wt % still remained.

2.2.4. Rheological behavior tests

The rheological characteristic that describes elastic components is the complex modulus G', which represents the material's total resistance to

deformation. It is also called storage modulus because it also defines the storage of the energy during the motion in the structure. High elasticity in terms of G' confers more resistance to applied force [20, 21]. In Fig. 14, as increasing frequency, HAc hydrogel shows monotaneous deformation, whereas composite hydrogels show linear deformation, indicating composites are stiffer than HAc hydrogel. Precipitated composite hydrogels exhibit improvement on rheological behaviors, indicating the shear moduli is 2.5 times as great as simply mixture hydrogel as shown in Fig. 15. In-situ precipitation enables strong incorporation of nanoparticles into a polymer matrix. Moreover, composite hydrogels exhibit improvement on rheological behaviors, indicating the shear moduli of composite hydrogels are 2.5-4 times as great as pure HAc hydrogel depending on the CaP content (Table 2).

2.2.5. *In vitro* cell tests

The *in vitro* cellular responses on the pure hydrogel and nanocomposite hydrogels were shown in Fig. 16. The cell morphology is

strongly related to biochemical function. In particular, rounded cell morphology is related to limited proliferation and cellular processed in the early stages of tissue formation [22]. Fibroblast cells show more polarized morphology throughout the nanocomposite hydrogels as compared to HAc hydrogel. The cells on the pure hydrogels maintained a rounded morphology whereas cells on the nanocomposite hydrogels were fully spread and exhibited a stretched shape suggesting a high motility activity. The improvement on cell attachment results from two reasons including the increasing effect on the hydrogel matrix stiffness and biocactive ceramics particles. CaP particles incorporated within the hydrogels can induce cellular stimulation.

In Fig. 17, the level of cell proliferation behaviors on the nanocomposite hydrogels after 5d was around 8 times higher than that on HAc hydrogel, implying the enhanced biocompatibility of composite hydrogels. In Fig. 18, Cells were also found to penetrate up to ~ 60 μm depth from the surface of the composite hydrogels, whereas only 10 μm from the surface of HAc hydrogel.

Bioactive CaP particles uniformly distributed throughout the 3-dimentional composite hydrogels induce beneficial effect on fibroblast cell penetration depth. Cell shape is strongly related to biochemical function. In particular, rounded cell morphology is correlated with limited proliferation and cellular processed in the early stages of tissue formation. It is expected that these nanocomposite hydrogels have high potential for use as skin tissue regeneration application due to its good biocompatibility in comparison to the pure HAc hydrogel.

2.3. Discussion

There have been numerous approaches to make hydrogel networks with improved mechanical properties. The composite hydrogels incorporated with nanoparticles for reinforcement were found in previous researches [10-12, 15, 23, 24]. In an attempt to overcome the limitation of HAc such as poor mechanical strength and low resistance to enzymatic degradation, we have introduced in-situ precipitation process to fabricate the nanocomposite HAc

hydrogel. It is distinguishable from the conventionally developed composites in terms of the fabrication method. Uniformly distributed and entangled CaP nanoparticles on HAc matrix affected the physical properties including the equilibrium swelling ratio, *in vitro* degradation and rheological behaviors.

The swelling ratio of the nanocomposites and the pure HAc hydrogel were summarized in Fig. 12. It was remarkable that the external pH causes influence on water absorption of the hydrogels. Since HAc hydrogel is an anionic-type superabsorbent material, it contains numerous dissociable hydrophilic –COOH and –COO- groups which can be ionized at high pH but unionized at low pH. At high pH, the gel networks can expand and hold more water molecules due to the electrostatic repulsion among the ionized -COO^- groups (COOH $\rightarrow$ COO^-) [25]. In acidic medium, there are relatively few free carboxyl groups in the HAc polymer chain. On the other hand, there are numerous negatively charged groups in the polymer matrix in the basic environment, leading to an increased equilibrium swelling ratio. The effect of

CaP nanoparticles content on the swelling kinetics of the nanocomposite hydrogels was also investigated. It was noticeable that the swelling degree was strongly dependent on the CaP concentration. It is attributed to the nanoparticles physically interacting with HAc and acting roles as filler which account for the empty space within the gel network. It leads to more compact and dense gel which cannot swell as much as pure HAc hydrogel [17].

According to the shear modulus as a function of frequency, the rheological behaviors of the nanocomposite hydrogels show that almost frequency-independent storage modulus. The curves run nearly parallel in the entire frequency range from 0.1 to 100 rad/s. And as increasing the CaP amounts within the hydrogels, the absolute value of G' increased due to the physically strengthened structures. In comparison, both G' of the original HAc hydrogel and the composite hydrogel fabricated by simple-mixing fall with decreasing frequencies. These results indicate that higher deformation is possible in a network of simply mixed composite hydrogel than

nanocomposite hydrogels due to weak interaction between mixed ceramic powders and HAc polymer chains. Moreoever it indicates that covalent cross-linking property of the HAc polymer itself dominated in the simply-mixed hydrogel [17]. In the case of the nanocomposite hydrogels, strong electrostatic interactions between nano particles and HAc polymer chains result in higher storage modulus. Nano CaP particles can be precipitated and strongly entangled on the nuclei sites formed by ionized COO- groups due to high pH level with ammonium hydroxide solution, which can be demonstrated as the chelating effect. Under basic conditions, the –COO- groups could chelate the Ca^{2+} and promote the nucleation of CaP [24, 26]. Due to the chelating effect throughout the hydrogel, CaP particles can be uniformly distributed in general and they also lead to high frictional force when the shear stress is applied on the nanocomposite hydrogels [27, 28]. Compared to the pure HAc gel and simply mixed composite gel, uniformly distribution and friction between particles-particles and particles-polymers are dominate impacts on the

rheological kinetics [29]. It is also deduced that the rheological properties can be tailored by modulating CaP particles content for various tissue engineering application.

However, the value G' of fully swollen nanocomposite hydrogels have different tendency in comparison with as prepared as shown in Fig. 15. When the nanocomposite hydrogels are fully swollen in PBS, nano particles content have little effect on rheological behaviors. The mechanical integrity of the swollen hydrogels became less resistant to change because the distance between CaP particles increased in water-rich environment. It is indicated that mobility restriction effect based on CaP amounts was significantly decreased in large amount of water content absorbed in hydrogel. The schematic diagram comparing the mechanism difference between the simply-mixing method and in-situ precipitation process was illustrated in Fig. 19. It can be also explained in terms of the decreased effective concentration of the swollen hydrogels compared to the concentration of the as-prepared.

It was also demonstrated that the enhancement of bioactivity by precipitating CaP particles resulting in highly stretched morphology and proliferation of the fibroblasts. It can be seen that the presence of CaP provided bioactive sites to the fibroblast cells [30-34]. The cell proliferation on the nanocomposite hydrogels directly correlated with the mechanical stiffness of the swollen gels regardless of the CaP content [35, 36]. Since the stiffness of the nanocomposite hydrogels from 10 to 40 wt % CaP amount exhibits within in the range of 200 Pa, fibroblast cells proliferate on a similar aspect.

2.4. Conclusion

From the in-situ precipitation, CaP-HAc nanocomposite hydrogels were successfully fabricated, where uniformly precipitated CaP nanoparticles were strongly entangled with HAc polymer chain. The composite hydrogels

exhibit significantly reduced degradation rates and dramatic improvement of shear modulus. The in vitro cell test results also demonstrated significantly enhanced biocompatibility of the composite hydrogels. By controlling the CaP amounts, mechanical and biological behaviors of the nanocomposite hydrogel can be optimized, exhibiting great potential for various biomedical applications.

Table 2. Shear modulus at 1 rad/s

CaP content (wt %)	As prepared (Pa)	After swollen (Pa)
0	95.55±4.15	40.07±7.02
10	243.8±49.9	140.0±49.0
20	297.7±30.9	129.4±24.7
30	347.8±35.0	150.1±41.6
40	512.2±70.2	195.4±17.7

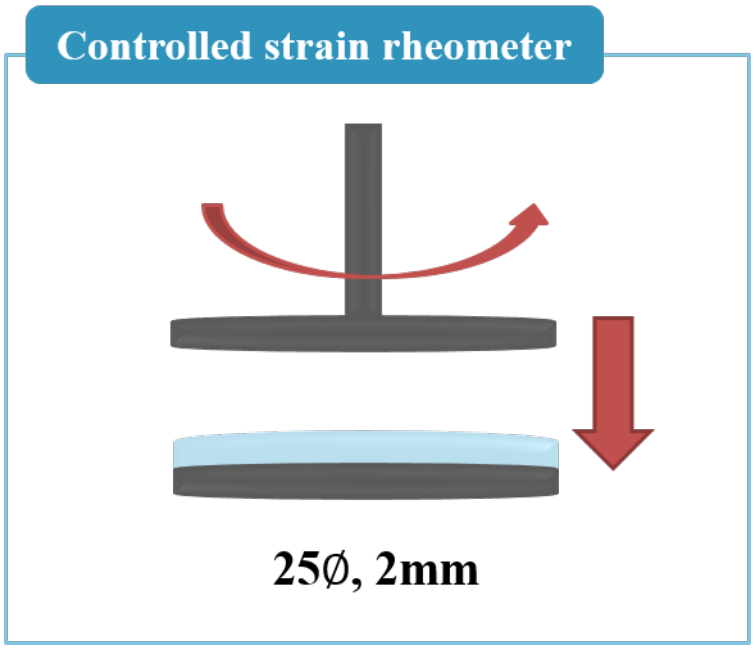

Figure 4. Schematic diagram for controlled strain rheometer.

Figure 5. Optical image of the hydrogels sample before and after implantation under dermis of the rats.

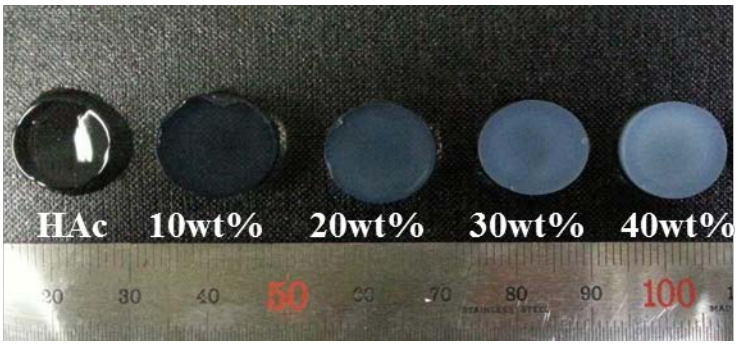

Figure 6. Optic image of the hydrogels (the original HAc hydrogel and the composite hydrogels with different CaP content.

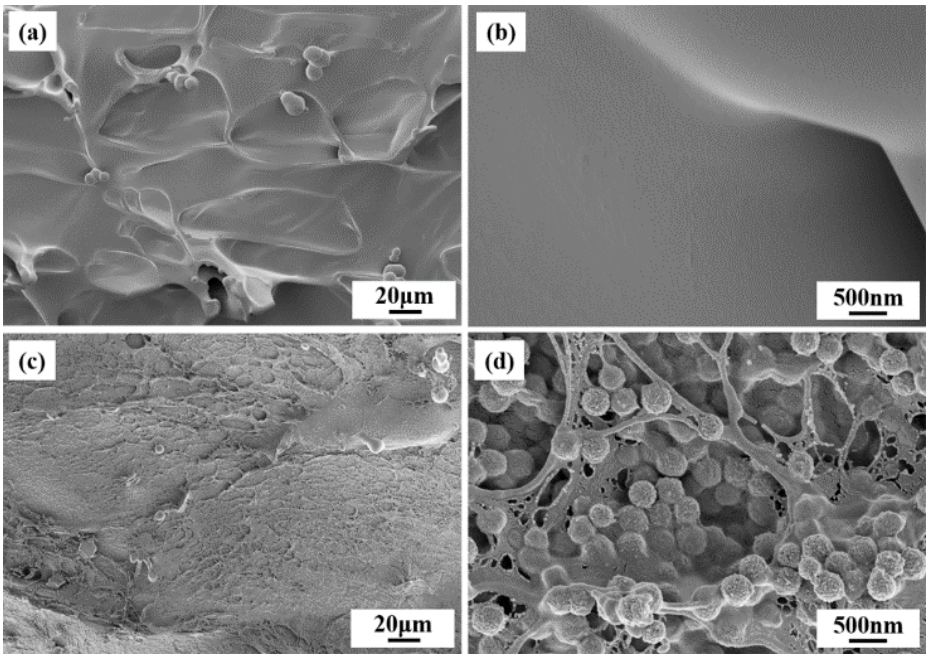

Figure 7. SEM images of (a,b) HAc and (c,d) nanocomposite hydrogel (30 wt%)

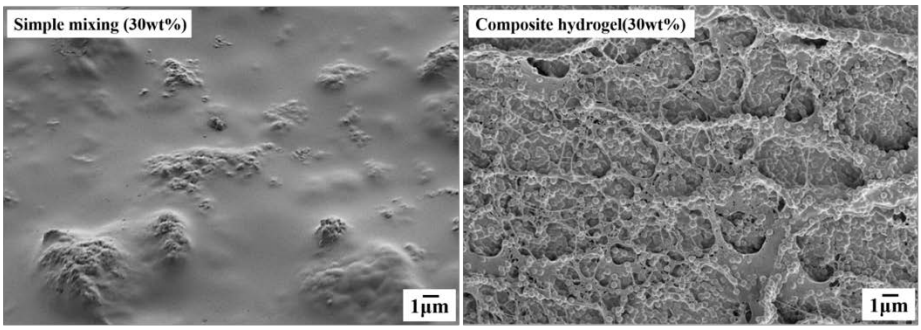

Figure 8. Optic image and Scanning electron microscopy (SEM) images of the simply mixed composite (left) and in-situ precipitated composite (right).

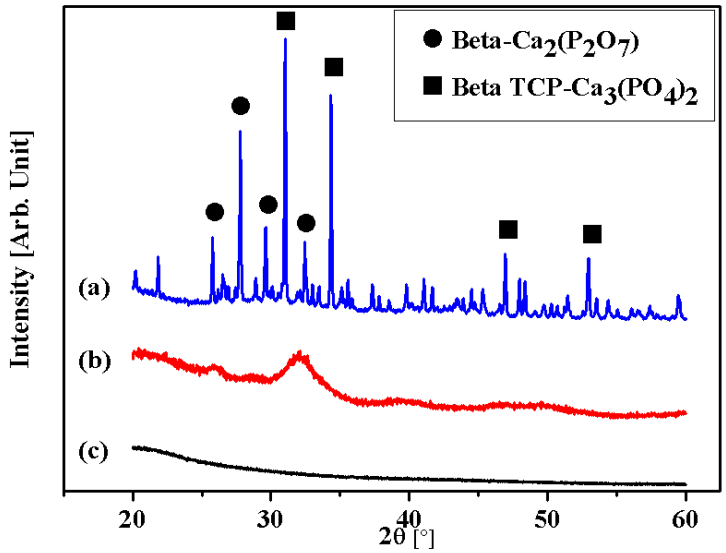

Figure 9. X-ray diffraction (XRD) patterns of (a) the HAc hydrogel, (b) the composite hydrogel and (c) the composite hydrogel with heat treatment.

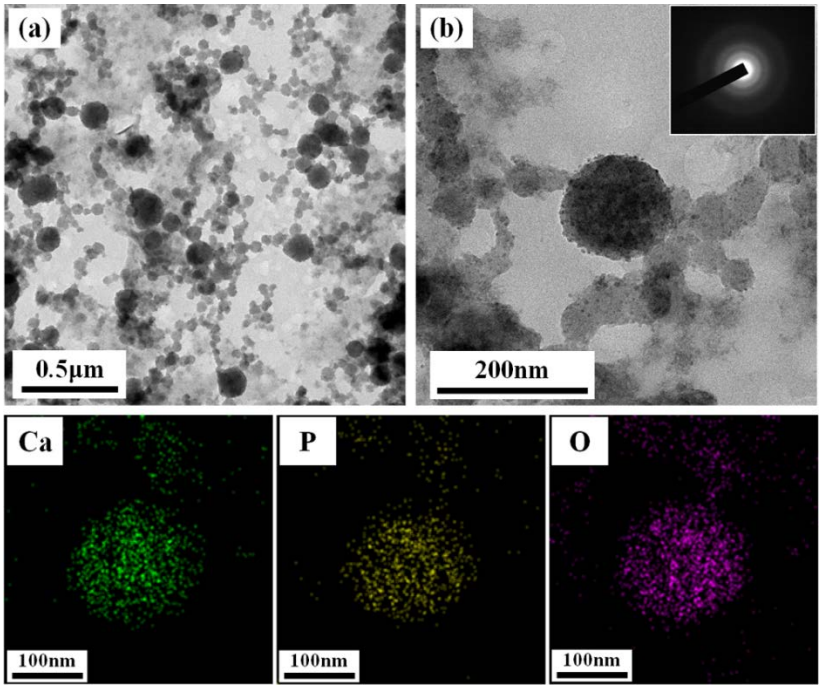

Figure 10. Transmission electron microscopy (TEM) images of the composite hydrogel.

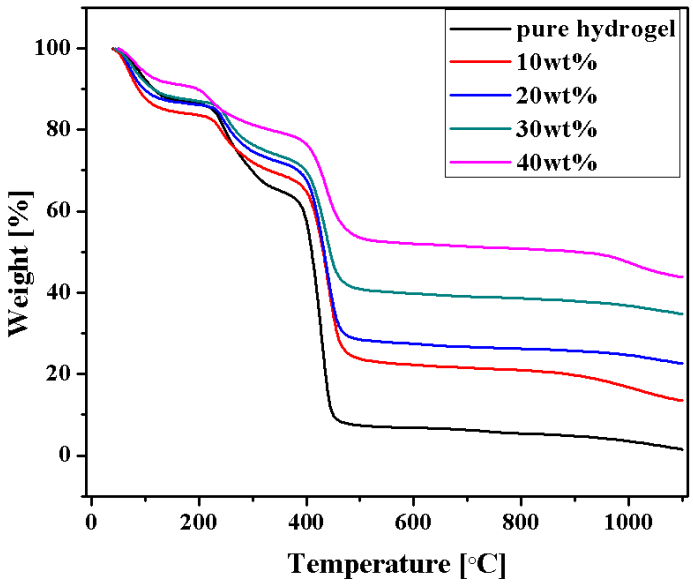

Figure 11. Thermal gravity analysis of the composite hydrogels.

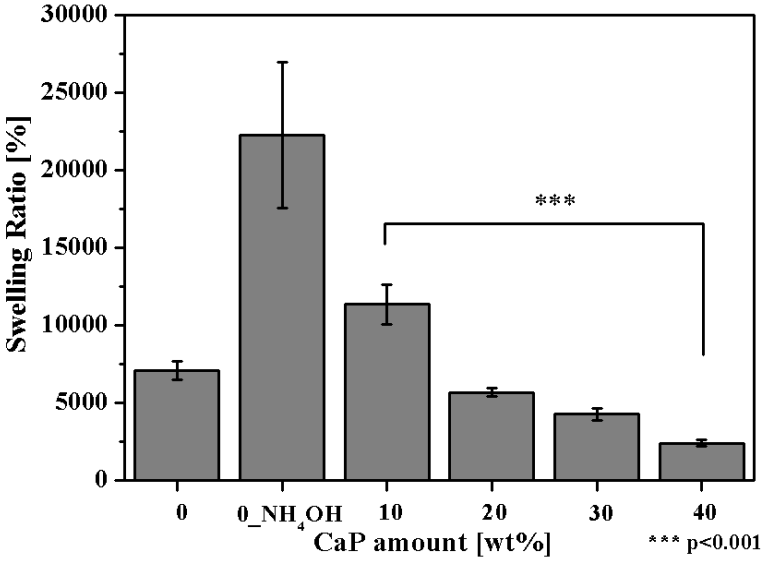

Figure 12. Swelling behaviors of the hydrogels with different CaP content.

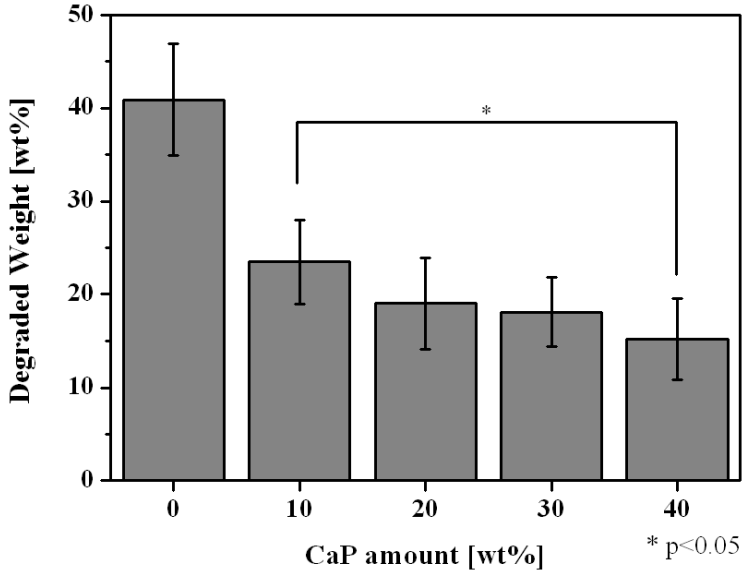

Figure 13. Degradation weight of the hydrogels with various CaP content.

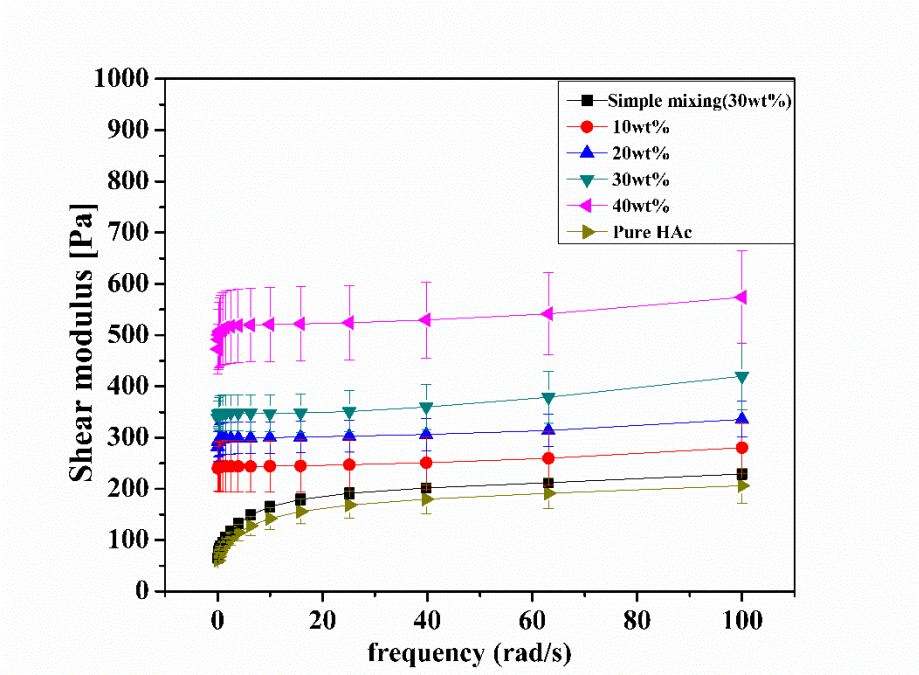

Figure 14. Rheological behaviors of as-prepared hydrogels at the range of frequency 0.1 to 100 rad/s.

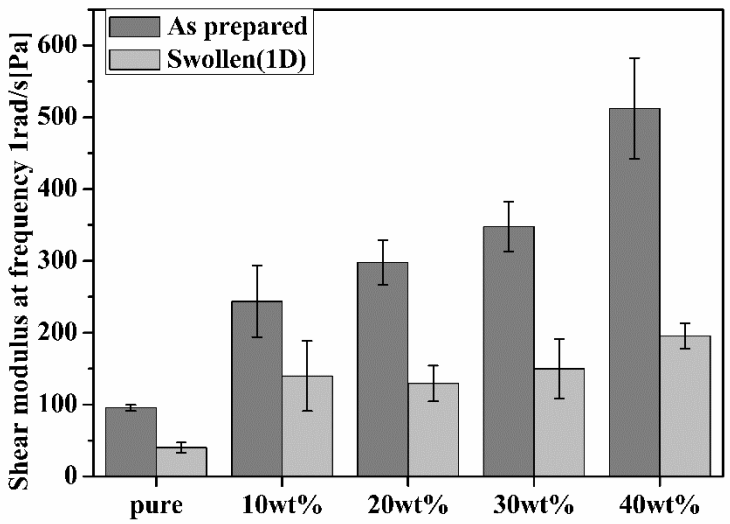

Figure 15. The comparison in terms of the shear modulus between as prepared and swollen states.

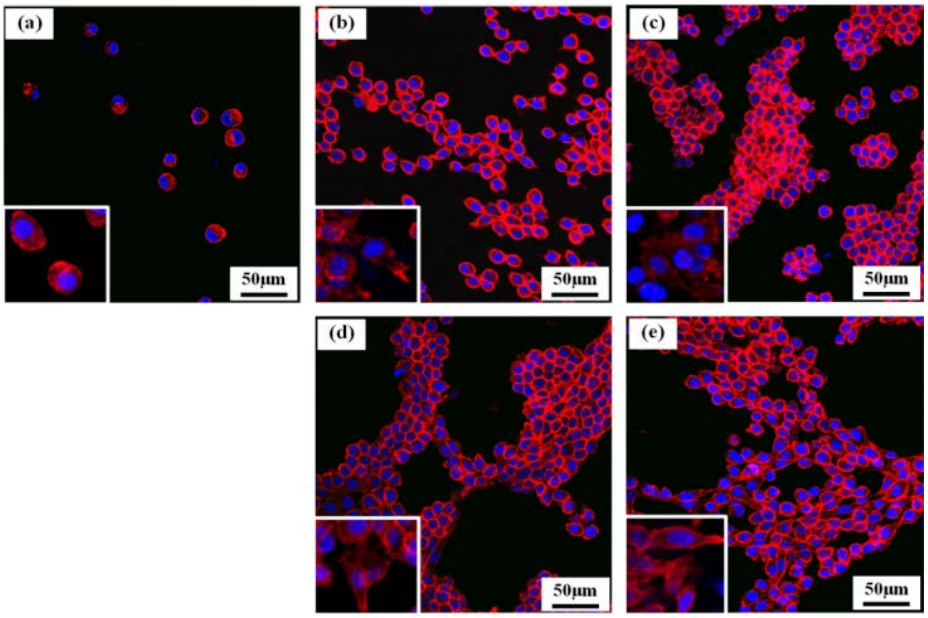

Figure 16. Confocal laser scanning images of the L929 cells that were cultured on the HAc hydrogel and the composite hydrogels for 3d.

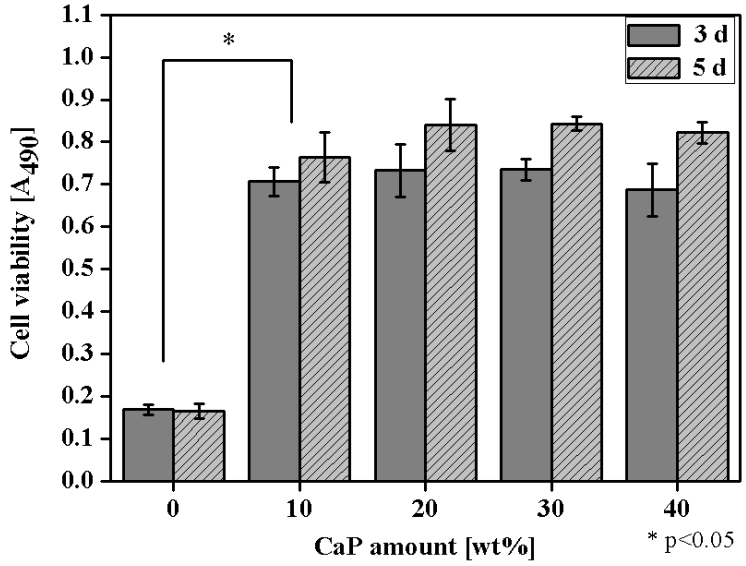

Figure 17. MTs assay after 3, 5d with various CaP content.

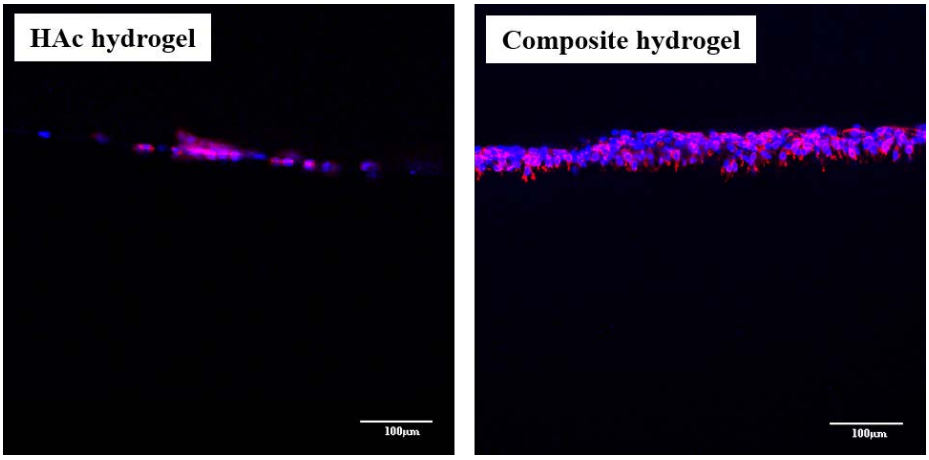

Figure 18. Confocal laser scanning images of the L929 cells that penetrated into the HAc hydrogel(left) and the nano composite hydrogels (right).

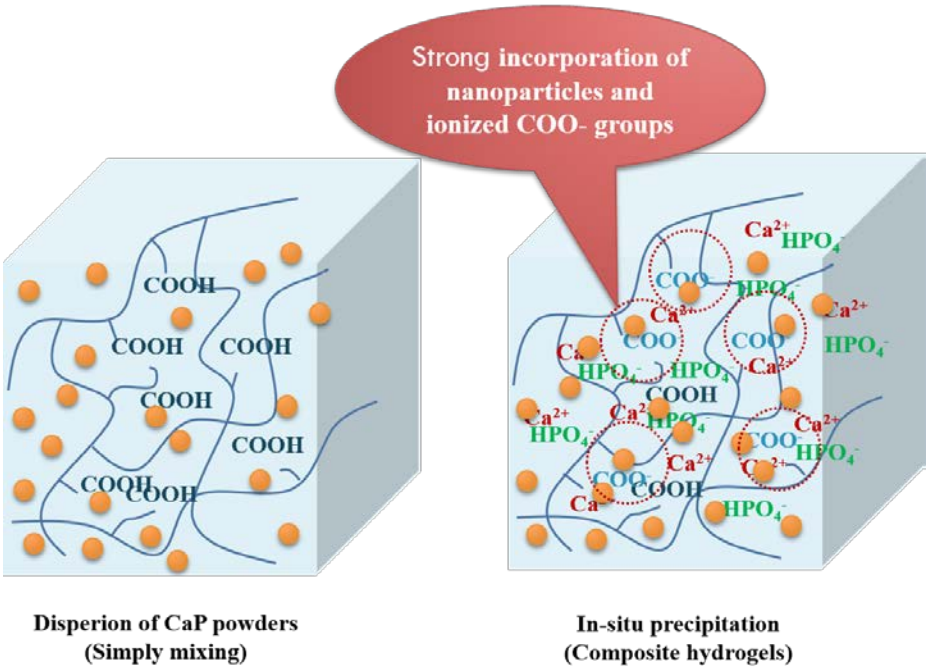

Figure 19. Schematic diagram explaining that in-situ precipitation enables homogenous and fast incorporation of nanoparticles into a polymer matrix producing nuclei cites.

Conclusion

In this study, we developed HAc-CaP nanocomposite hydrogels to make up for the weak points of hyaluronic acid hydrogel itself in terms of poor biomechanical properties and fast enzymatic degradation. It can be easily fabricated varying the CaP content to modulate different physical and biochemical traits. It was shown that CaP particles can be strongly incorporated with the HAc hydrogel via in-situ precipitation process, uniformly distributed in nano scale. Homogenous distribution throughout the 3-dimentional polymer matrix induces dramatic improvement of elastic modulus and significant retarded degradation rates. The CaP nanoparticles also accelerate the early stages of cellular response on the composite hydrogel demonstrating significantly enhanced biocompatibility. In vivo results with better cell penetration and high density of collagen formation also indicate the potential for use as a connective tissue regenerative scaffold. Future studies in terms of the growth factor carrier can be carried out for further advances in the field of regenerative tissue engineering.

References

[1] Xu X, Jha AK, Harrington DA, Farach-Carson MC, Jia XQ. Hyaluronic acid-based hydrogels: from a natural polysaccharide to complex networks. Soft Matter. 2012;8:3280-94.

[2] Dhandayuthapani B, Yoshida Y, Maekawa T, Kumar DS. Polymeric Scaffolds in Tissue Engineering Application: A Review. Int J Polym Sci. 2011.

[3] Striedner J, Geissler S, Czygan FC, Braunegg G. Contributions to the Biotechnological Production of Sweeteners from Stevia-Rebaudiana Bertoni .3. Accumulation of Secondary Metabolites by Means of a Precursor and by Elicitation of Cell-Cultures. Acta Biotechnol. 1991;11:505-9.

[4] Segura T, Anderson BC, Chung PH, Webber RE, Shull KR, Shea LD. Crosslinked hyaluronic acid hydrogels: a strategy to functionalize and pattern. Biomaterials. 2005;26:359-71.

[5] Hahn SK, Park JK, Tomimatsu T, Shimoboji T. Synthesis and degradation test of hyaluronic acid hydrogels. Int J Biol Macromol. 2007;40:374-80.

[6] Bencherif SA, Srinivasan A, Horkay F, Hollinger JO, Matyjaszewski K, Washburn NR. Influence of the degree of methacrylation on hyaluronic acid hydrogels properties. Biomaterials. 2008;29:1739-49.

[7] Hachet E, Van Den Berghe H, Bayma E, Block MR, Auzely-Velty R. Design of Biomimetic Cell-Interactive Substrates Using Hyaluronic Acid

Hydrogels with Tunable Mechanical Properties. Biomacromolecules. 2012;13:1818-27.

[8] Collins MN, Birkinshaw C. Physical properties of crosslinked hyaluronic acid hydrogels. J Mater Sci-Mater M. 2008;19:3335-43.

[9] Monheit GD, Baumann LS, Gold MH, Goldberg DJ, Goldman MP, Narins RS, et al. Novel Hyaluronic Acid Dermal Filler: Dermal Gel Extra Physical Properties and Clinical Outcomes. Dermatol Surg. 2010;36:1833-41.

[10] Dickerson MB, Sandhage KH, Naik RR. Protein- and Peptide-Directed Syntheses of Inorganic Materials. Chem Rev. 2008;108:4935-78.

[11] Gaharwar AK, Schexnailder PJ, Jin Q, Wu CJ, Schmidt G. Addition of Chitosan to Silicate Cross-Linked PEO for Tuning Osteoblast Cell Adhesion and Mineralization. Acs Appl Mater Inter. 2010;2:3119-27.

[12] Gaharwar AK, Schexnailder PJ, Dundigalla A, White JD, Matos-Perez CR, Cloud JL, et al. Highly Extensible Bio-Nanocomposite Fibers. Macromol Rapid Comm. 2011;32:50-7.

[13] Gaharwar AK, Schexnailder PJ, Kline BP, Schmidt G. Assessment of using Laponite (R) cross-linked poly(ethylene oxide) for controlled cell adhesion and mineralization. Acta Biomater. 2011;7:568-77.

[14] Haraguchi K, Takehisa T. Nanocomposite hydrogels: A unique organic-inorganic network structure with extraordinary mechanical, optical, and swelling/de-swelling properties. Adv Mater. 2002;14:1120-4.

[15] Shi XF, Hudson JL, Spicer PP, Tour JM, Krishnamoorti R, Mikos AG. Injectable nanocomposites of single-walled carbon nanotubes and

biodegradable polymers for bone tissue engineering. Biomacromolecules. 2006;7:2237-42.

[16] Yokoi T, Kawashita M, Kikuta K, Ohtsuki C. Biomimetic mineralization of calcium phosphate crystals in polyacrylamide hydrogel: Effect of concentrations of calcium and phosphate ions on crystalline phases and morphology. Mat Sci Eng C-Mater. 2010;30:154-9.

[17] Gaharwar AK, Dammu SA, Canter JM, Wu CJ, Schmidt G. Highly Extensible, Tough, and Elastomeric Nanocomposite Hydrogels from Poly(ethylene glycol) and Hydroxyapatite Nanoparticles. Biomacromolecules. 2011;12:1641-50.

[18] Schramm C, Spitzer MS, Henke-Fahle S, Steinmetz G, Januschowski K, Heiduschka P, et al. The Cross-linked Biopolymer Hyaluronic Acid as an Artificial Vitreous Substitute. Invest Ophth Vis Sci. 2012;53:613-21.

[19] Burdick JA, Chung C, Jia XQ, Randolph MA, Langer R. Controlled degradation and mechanical behavior of photopolymerized hyaluronic acid networks. Biomacromolecules. 2005;6:386-91.

[20] Tezel A, Fredrickson GH. The science of hyaluronic acid dermal fillers. Journal of Cosmetic and Laser Therapy. 2008;10:35-42.

[21] Sundaram H, Voigts B, Beer K, Meland M. Comparison of the Rheological Properties of Viscosity and Elasticity in Two Categories of Soft Tissue Fillers: Calcium Hydroxylapatite and Hyaluronic Acid. Dermatol Surg. 2010;36:1859-65.

[22] Chicurel ME, Chen CS, Ingber DE. Cellular control lies in the balance of forces. Curr Opin Cell Biol. 1998;10:232-9.

[23] Hu YY, Rawal A, Schmidt-Rohr K. Strongly bound citrate stabilizes the apatite nanocrystals in bone. P Natl Acad Sci USA. 2010;107:22425-9.

[24] Jiao Y, Gyawali D, Stark JM, Akcora P, Nair P, Tran RT, et al. A rheological study of biodegradable injectable PEGMC/HA composite scaffolds. Soft Matter. 2012;8:1499-507.

[25] Wang W, Wang A. Preparation, swelling and water-retention properties of crosslinked superabsorbent hydrogels based on guar gum. 2010. p. 177-82.

[26] Li QH, Li M, Zhu PZ, Wei SC. In vitro synthesis of bioactive hydroxyapatite using sodium hyaluronate as a template. J Mater Chem. 2012;22:20257-65.

[27] Chiou BS, Raghavan SR, Khan SK. Effect of colloidal fillers on the cross-linking of a UV-curable polymer: Gel point rheology and the Winter-Chambon criterion. Macromolecules. 2001;34:4526-33.

[28] Habraken WJEM, Wolke JGC, Jansen JA. Ceramic composites as matrices and scaffolds for drug delivery in tissue engineering. Adv Drug Deliver Rev. 2007;59:234-48.

[29] Nickerson CS, Park J, Kornfield JA, Karageozian H. Rheological properties of the vitreous and the role of hyaluronic acid. J Biomech. 2008;41:1840-6.

[30] Li ZY, Su YL, Xie BQ, Wang HL, Wen T, He CC, et al. A tough hydrogel-hydroxyapatite bone-like composite fabricated in situ by the electrophoresis approach. J Mater Chem B. 2013;1:1755-64.

[31] Kontonasaki E, Sivropoulou A, Papadopoulou L, Garefis P, Paraskevopoulos K, Koidis P. Attachment and proliferation of human

periodontal ligament fibroblasts on bioactive glass modified ceramics. J Oral Rehabil. 2007;34:57-67.

[32] Baxter LC, Frauchiger V, Textor M, Ap Gwynn I, Richards RG, Bongrand P, et al. Fibroblast and osteoblast adhesion and morphology on calcium phosphatesurfaces. European Cells and Materials. 2002;4:1-17.

[33] Kutty JK, Cho E, Lee JS, Vyavahare NR, Webb K. The effect of hyaluronic acid incorporation on fibroblast spreading and proliferation within PEG-diacrylate based semi-interpenetrating networks. Biomaterials. 2007;28:4928-38.

[34] Bongio M, van den Beucken JJJP, Nejadnik MR, Leeuwenburgh SCG, Kinard LA, Kasper FK, et al. Biomimetic modification of synthetic hydrogels by incorporation of adhesive peptides and calcium phosphate nanoparticles: In vitro evaluation of cell behavior. European Cells and Materials. 2011;22:359-76.

[35] Banerjee A, Arha M, Choudhary S, Ashton RS, Bhatia SR, Schaffer DV, et al. The influence of hydrogel modulus on the proliferation and differentiation of encapsulated neural stem cells. Biomaterials. 2009;30:4695-9.

[36] Bott K, Upton Z, Schrobback K, Ehrbar M, Hubbell JA, Lutolf MP, et al. The effect of matrix characteristics on fibroblast proliferation in 3D gels. Biomaterials. 2010;31:8454-64.

초 록

본 논문은 히알루론산 하이드로겔 내부에 생체특성이 좋은 나노 입자 크기의 인산칼슘을 석출시켜 기존 하이드로겔보다 기계적 물성 및 팽윤 정도와 분해되는 다양한 물리적 특성을 향상시키는 연구에 대하여 다루었다.

고분자 용액과 세라믹 입자를 교반하여 제작한 기존 하이드로겔 복합체 연구에서는 상대적으로 무거운 세라믹 입자가 가라앉아 분리가 일어나 균일한 복합체를 만들기가 어렵고 두 물질의 상호작용이 매우 약하여 물리적 특성 향상정도가 낮다는 단점이 있다. 이를 해결하기 위해 하이드로겔을 인산칼슘의 전구체인 염화칼슘과 인산용액에 두어 이온이 내부로 확산되게 한 후 수산화암모늄으로 인산칼슘 석출을 시켜 하이드로겔 복합체를 제작하였다.

실험을 통하여 얻은 복합체내 석출된 인산칼슘 입자의 미세구조를 관찰하고 팽윤정도와 효소에 의한 분해정도 차이를 측정하고 하이드로겔 복합체의 유변학적 물성 평가를 수행하였다. 그리

고 생체특성평가를 위해 섬유아세포를 이용하여 세포부착 및 세포 증식 평가를 진행하였다.

석출과정을 통해 생성된 인산칼슘 입자들이 음전하로 이온화된 히알루론산 구조에 강력한 정전기적 인력으로 존재하며 이 또한 고르게 분산되어 있음을 확인하였다. 이로 인해 히알루론산 하이드로젤의 습윤능력 및 효소에 의한 분해정도를 인산칼슘 조성에 따라 다양하게 조절이 가능한 것으로 보였다. 유변학적 물성 면에서도 단순히 세라믹 입자를 교반하여 만든 복합체와는 전혀 다른 고체에 가까운 물성을 나타내었다. 교반하여 만든 복합체보다 2.5배 강한 나노복합체를 제작할 수 있음을 확인하였다. 이는 고르게 분산된 인산칼슘의 강한 마찰력으로 인하여 생긴 결과라고 볼 수 있다. 또한, 생체특성이 좋은 인산칼슘의 존재로 인하여 섬유아세포의 부착정도와 증식정도가 상당히 향상되는 것을 알 수 있었다. 인산칼슘 입자 조성에 따른 증식정도는 크게 비례하지 않고 비슷한 수준의 증식수준을 나타내었다.

현재 진행중인 동물실험을 통하여 필러 및 연조직 재생용 스캐폴드로써의 가능성을 확인할 예정이다. 향후 과제로는 히알루론산 나노복합체에 FGF-2(fibroblast growth factor)성장인자를 담지하여 서방형 방출을 함으로써 연조직 재생 응용을 위한 연구를 진행할 예정이다.

주요어: 히알루론산, 석출과정, 나노 인산칼슘입자, 생체적합성, 섬유아세포

학 번: 2012-20632